Optimizing Radiation Therapy Treatments by Exploring Tumour Ecosystem Dynamics in – silico

Stephan Scheidegger[1] and Harold Fellermann[2]

[1]ZHAW School of Engineering, Zurich University of Applied Sciences, Winterthur, Switzerland
[2]Interdisciplinary Computing and Complex Biosystems Research Group, School of Computing, Newcastle University, Newcastle upon Tyne, UK
scst@zhaw.ch

Abstract

In this contribution, we propose a system-level compartmental population dynamics model of tumour cells that interact with the patient (innate) immune system under the impact of radiation therapy (RT). The resulting *in silico* - model enables us to analyse the system-level impact of radiation on the tumour ecosystem.

The Tumour Control Probability (TCP) was calculated for varying conditions concerning therapy fractionation schemes, radio-sensitivity of tumour sub-clones, tumour population doubling time, repair speed and immunological elimination parameters. The simulations exhibit a therapeutic benefit when applying the initial 3 fractions in an interval of 2 days instead of daily delivered fractions. This effect disappears for fast-growing tumours and in the case of incomplete repair. The results suggest some optimisation potential for combined hyperthermia-radiotherapy.

Regarding the sensitivity of the proposed model, cellular repair of radiation-induced damages is a key factor for tumour control. In contrast to this, the radio-sensitivity of immune cells does not influence the TCP as long as the radio-sensitivity is higher than those for tumour cells. The influence of the tumour sub-clone structure is small (if no competition is included). This work demonstrates the usefulness of *in silico* – modelling for identifying optimisation potentials.

Introduction

Cancer remains to be one of the most elusive widespread diseases – accounting for an estimated 16% of worldwide deaths.[1] In the last decades, many improvements concerning equipment and treatment planning tools have driven anti-cancer radiation therapy (RT) towards precise applications of radiation doses. Remarkable progress has been made regarding geometrical precision. In contrast to these more engineering – related aspects, the biological knowledge about growth dynamics and therapy response of tumours seems to remain behind technology development. This may be a reason for the upcoming discussion of a biologically adapted RT (Thorwarth, 2017).

One of the reasons for the comparably slow progress of biological understanding lies in the differences between the behaviour of tumour cells in vitro, in vivo (mouse model) and in patient, which, on the one hand, prevent a direct transfer of knowledge gained by experiments to clinical treatment, and on the other hand, indicate that cancer is a systemic disease that can only be understood by treating tumours as complex systems that are intricately coupled to their host environment including the immune system.

Several studies consequently hypothesize that the major cause of radio-resistance observed during RT treatments may be related to the heterogeneity of tumour tissues (Horsman et al., 2012; Baumann et al., 2016). Under this systemic perspective, cancer might be regarded as an evolving ecosystem of diverse cell populations (different tumour sub-populations or sub-clones, host tissue, endothelial cells / vascular system, immune cells) with a dynamic behaviour influenced by the boundary conditions of RT. In such a framework, radiation-induced cell killing would constitute a selection pressure that leads to survival of radio-resistant sub-populations. Loss of competition between the different cancer sub-populations and host tissue might lead to an accelerated progress of disease. Evolutionary dynamics of cancer (Crespi & Summers, 2005) could be responsible for an adapted response of the tumour to anti-cancer therapy.

Ecological aspects of anti-cancer therapy have been discussed by different authors (Pienta et al., 2008; Basanta et al. 2015; Basanta et al., 2012). Merlo et al. (2006) considered cancer as an evolutionary and ecological process. Gatenby et al. pointed out the role of evolutionary dynamics for cancer prevention (Gatenby et al., 2010). Ecological principles have also motivated the investigation of the invasion of metastasizing cancer cells into bone marrow (Chen & Pienta, 2011). The connection between artificial life and cancer research has been pioneered by Maley and Forrest (2000) who developed an agent based model of precancerous cells that might develop into cancer by adopting mutations at atypically high rate. Population dynamics of tumours have been further studied by Gonzales-Garcia et al. (2002) and Sole (2003) who concluded through agent-based modelling that spatial genetic heterogeneity observed in tumours naturally follows from simple ecological competitor dynamics. Since then, many multi-agent models of tumour growth with increasing physical accuracy have been proposed (Abbott et al. 2006, Zhang et al. 2009, Bentley 2013, Ozik et al. 2018 and others). Yet, few of these approaches take into account the dynamics of and interaction with the tumour environment, particularly host

[1] https://ourworldindata.org/causes-of-death

tissue, immune system, and boundary conditions imposed by anti-cancer therapies.

Scheidegger et al. (2010) demonstrated by a combined population model *in silico* that - in certain situations - the tumour response to radiation is dominated by the radio-sensitivity of the endothelial cells. In the light of these results, there is certain evidence that tissue dynamics could play a pivotal role in development and therapy response of tumours. Scott et al. (2016) investigated the impact of spatial metrics onto the radiation efficacy using a hybrid cellular automaton model.

Despite this increased appreciation of ecological and evolutionary aspects of cancer dynamics, relatively little work has been performed that attempts to transfer well-established methodological approaches from theoretical ecosystem analysis to the domain of RT.

We here propose a high-level population dynamics model of tumour cell populations that interact with a simplified immune system under the impact of RT treatment (Fig. 1).

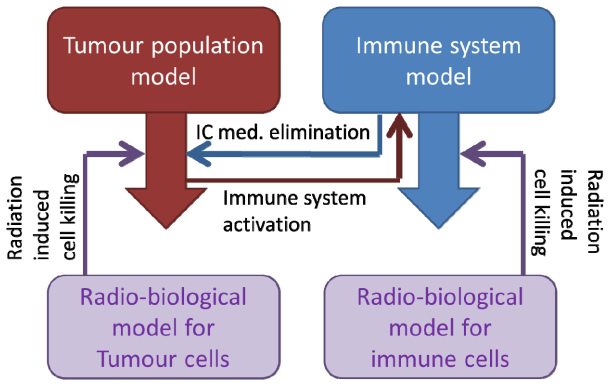

Figure 1: Structure with the different sub-models of a simplified tumour - immune system model. IC med. elimination means immune cell mediated cell killing.

Due to the shear complexity of the biological tumour system and its response to both, the immune system and RT, we regard it as unpromising to bring the mechanistic details of the tumour ecosystem into a computer model: many of details are un-known and quantifiable experimental insight into most of the different dynamic processes is missing. Therefore, we propose a system dynamics-based phenomenological model, in order to support hypothesis generation and design of experiments in vitro or clinical trials. While our approach sacrifices many of the mechanistic details underlying tumour growth and treatment, the model has been developed with clinical applicability in mind: model parameters are in principle measurable and chosen to represent realistic parameter ranges, and model predictions are reported through clinically meaningful quantifiers.

By improving the systemic understanding of tumour ecosystems, quantitative *in silico* analysis of system-level cancer models could subsequently help to improve or optimize anti-cancer treatment strategies. This broadened ecological and evolutionary view on the impact of RT onto tumours could be an important step for understanding the dynamics responsible for treatment response and may serve as a basis to optimize and improve RT treatments.

In this work, we will focus on the optimisation potential regarding fractionation schemes in External Beam Radiation Therapy (EBRT). In case of an EBRT, the radiation is applied by fractions with a dose per fraction of e.g. 2 Gy for prostatic adenocarcinoma (Fowler et al., 1995). Typically, the standard fractionation scheme for EBRT for adeno-carcinomas is a daily application of the fractions (5 days per week). There is a recent discussion about hypo-fractionation (less fractions with a higher radiation dose) for example using daily fraction doses of 2.75 Gy (e.g. non-small lung cancer; De Dios et al. 2017). Arguments for choosing a fractionated application are related to the 4 R's in RT: **R**epair (host tissue has faster repair compared to tumour cells, fractionation leads to a larger, so called "therapeutic window"), **R**epopulation (longer interval will allow tumours to repopulate), **R**e-oxygenation (reduction of tumour mass will enhance oxygenation and therefore increase radio-sensitivity of the tumour cells for subsequent fractions) and **R**edistribution (mitotic cells are more radio-sensitive and radiation-induced cell killing can cause a synchronisation of tumour cells regarding the cell cycle). Fraction size and time interval between fractions should be optimised: long intervals lead to unwanted tumour growth and complete repair of tumour cells, short intervals to less re-oxygenation and decreasing difference between cellular repair of tumour cells and host tissue (smaller therapeutic window). It has to be pointed out here that this is only a simplified explanation, not referring to the full ecosystem dynamics and excluding the aspect of immune system interaction. Exploring artificial life *in silico* could support modelling the immune system interaction and improve the understanding of the complex dynamics including pattern recognition.

Materials and Methods

The model describes tumour cell populations $T_k = T_k(t)$ interacting with an immune cell population $M = M(t)$. Both, immune cells and tumour cells are considered to be radio-sensitive. For modelling the radiation-induced elimination, a simplified Γ-LQ-model is applied (Scheidegger et al. 2011a). In this model, the elimination rate of tumour cell is determined by the radio-sensitivity constants α and β (which are considered to be population-specific) and the radiation dose rate R:

$$\left[\frac{dT_k}{dt}\right]_{Rad} = -\left(\alpha_k + 2\beta_k \Gamma_k\right) \cdot R \cdot T_k \qquad (1)$$

and for the immune cells:

$$\left[\frac{dM}{dt}\right]_{Rad} = -\left(\alpha_M + 2\beta_M \Gamma_M\right) \cdot R \cdot M \qquad (2)$$

The dose equivalent Γ (Transient Biological Dose Equivalent TBDE, the unit is Gray (Gy)) is rising with the dose rate R and decaying with cellular repair:

$$\frac{d\Gamma_{k,M}}{dt} = R - f(\Gamma_{k,M}) \quad (3)$$

In contrast to the full Γ-LQ-model (Scheidegger et al. 2011a), dose rate dependence is not considered (fixed dose rate) and repair is switched off during irradiation. Integration of Eq.3 leads to the well-established linear-quadratic model, where the logarithm of the surviving fraction S is given by a linear and a quadratic term of the radiation dose D: $\log S = -(\alpha D + \beta D^2)$. For repair, first order kinetics is assumed: $f(\Gamma_{k,M}) = \gamma_{k,M}\Gamma_{k,M}$. For the tumour cells (TBDE = Γ_k), two cases are examined: Complete repair - is assumed when the remaining dose equivalent (TBDE) is smaller than 1 mGy – and incomplete repair (TBDE ≥ 1mGy).

The growth of the tumour cell populations is determined by a growth constant k_T which is here chosen to be constant for all populations (sub-clones). Tumour cells can mutate with the rate $k_{mut}T_k$ to form or join another tumour sub-clone T_{k+1}. In addition to the radiation-induced elimination, tumour cells can be eliminated by the immune cells M. The development of the population size of the tumour cell population T_k is given by:

$$\frac{dT_k}{dt} = k_T T_k + k_{mut}(T_{k-1} - T_k) - w_k k_{ime,k} T_k M - \left[\frac{dT_k}{dt}\right]_{Rad} \quad (4)$$

w_k is an immune-response specific weighting factor for the population k. Different weights can be explained by the fact that the immuno-biological sensitivity may be influenced by the mutation in two ways: (*i*) Higher sensitivity is gained by an increased genetic instability of tumour cells collecting more mutations and (*ii*) decreasing immuno-sensitivity can be achieved by an evolutionary process due to immune-system driven selection of tumour cells expressing less detectable antigens on their surface (immunoediting by immune system (Vesely et al. 2011); escape from the immune response by reduction of self-antigen presenting Class I Major Histocompability Complex MHC).

Tumour cells that have been eliminated from the population T_k are transformed to apoptotic or necrotic cells N_k. These cells - and with them, the amount of radiation induced Damage Associated Membrane Proteins DAMP's (Grimsley et al., 2003) - can be eliminated by apoptosis and phagocytosis:

$$\frac{dN_i}{dt} = \left[\frac{dT_i}{dt}\right]_{Rad} - k_{rie} M N_k \quad (5)$$

In this model, no explicit pathway (apoptotic or necrotic, s. discussion) is chosen. *In vivo*, apoptotic cells are removed by macrophages, whereas necrosis may be accompanied by inflammation, leading to a more complex immune response. Natural killer cells can respond in absence of self-antigen presenting MHC and may be activated by DAMP's. DAMP's such as Heat Shock Proteins HSP (Srivastava, 2002, Daugaard et al., 2007) can be produced by ionizing radiation and are thus expressed in higher levels after RT (Nytko et al., 2019). The presented *in silico* model includes only one immune cell population. For simplicity, the activation of the (innate) immune system is assumed to be governed by the abundance of DAMP's in the tumour compartment, leading to an invasion of immune cells until an equilibrium level (or response level) M_{resp} is reached. Immune cells can be eliminated by radiation in the tumour compartment during RT. In consequence, the immune cell population in the tumour compartment is described by:

$$\frac{dM}{dt} = k_M \cdot \left(M_{resp} - M\right) - \left[\frac{dM}{dt}\right]_{Rad} \quad (6)$$

The DAMP-activation of the response level M_{resp} is assumed to be dependent on the sum of damaged cells by the following model:

$$M_{resp} = M_{\min} + M_{\max} \cdot \left(1 - e^{-r \cdot \sum_k N_k}\right) \quad (7)$$

$M_{\min}$ and $M_{\max}$ are limiting the amplitude of the response to a range between a minimal concentration ($M_{\min}$ per tumour compartment volume) of immune cells and a saturation level. Both levels may be dependent on patient specific immune response capability.

For clinical evaluation of the RT treatments, the Tumour Control Probability (TCP) is a well-established quantity. The TCP is calculated in the following way:

$$TCP = e^{-\sum_k T_k} \quad (8)$$

The concept behind Eq.8 is based on the fact that the description using differential equations delivers average population sizes. For small amounts of cells, statistical variation has to be taken into consideration.

In this study, EBRT was simulated by 32 fractions, each fraction with a radiation dose of 2.5 Gy. The fractionation schemes differ by the interval between the applications of RT fractions. A scheme with daily application was compared to fractionation with larger intervals of 2-4 days and a mixed scheme, where the initial 3 fractions have a spacing of 2 days, followed by daily application of subsequent fractions.

The simulations were carried out by numerical integration using a 4th order Runge-Kutta algorithm. The time increment was set to $\Delta t = 10^{-5}\,\mathrm{d}^{-1}$.

Results

Parameters used for the different simulations are summarized in Tab.1. The resulting TCP's are displayed in Fig. 2 and Fig. 3. In general, the selection of the parameter values is made in

regard to the resulting TCP: The parameter values are restricted to a range which results in a rising TCP (0.01 < TCP < 0.99) between a dose of 35 Gy and 80 Gy. This represents more or less the clinical observations for the selected radio-biological parameters.

	Parameter values	
Diagram No.	Fig.2	Fig.3
α_M /Gy^{-1}	0.5	0.5
β_M /Gy^{-2}	0.2	0.2
α_k / Gy^{-1}	varying	0.310 (k=1)
β_k / Gy^{-2}	varying	0.0625 (k=1)
γ_k/ d^{-1}	10 (for all k)	varying
k_T / d^{-1}	$3.46\cdot10^{-2}$ except. Fig. 2d	$3.46\cdot10^{-2}$
k_{mut} / d^{-1}	$5\cdot10^{-3}$	$5\cdot10^{-3}$
k_{rie} / d^{-1}	10^{-8}	10^{-8}
k_{ime} / d^{-1}	10^{-9}, varying for sub-clones	varying
k_M / d^{-1}	1	1
M_{min}	10^6	10^6
M_{max}	10^9	varying
r	10^{-3}	10^{-3}

Table 1: Parameter values used for the simulations: α and β for the tumour are in the upper range, especially when comparing to clinical studies but these values and the α/β-ratios are strongly varying across different patients and tumours (van Leeuwen et al., 2018); k_T is corresponding to an intrinsic tumour doubling time of 20 d (for clinical observed doubling times s. Mehrara et al., 2007).

The sensitivity of the model regarding the radio-biological parameters of the immune cells have been investigated by simulations using different α_M –and β_M – values: For simulations with the parameter set of Fig. 2, varying α_M – values do not have a significant impact on the TCP (less than 1%), as long as α_M > 0.3 Gy^{-1}. This is also the case for varying γ_M-values (set to 10 d^{-1}; invading immune cells are considered as not pre-irradiated).

In a first step, the influence of different tumour cell populations on the dynamics of the system is investigated. In Fig. 2, different scenarios regarding the radio-sensitivity and immunological interactions of tumour sub-clones (5 different populations) are shown. The simulation included a phase of tumour evolution during 300 days before start of RT. The initial population size was set to 10^9 cells, leading to approx. $3\cdot10^{12}$ tumour cells at the beginning of the treatment. It was assumed that all populations have a doubling time of 20 days (accordingly k_T = $3.46\cdot10^{-2}$ d^{-1}).

In Fig. 2a & 2b, the tumour sub-clones are considered to become more radio-sensitive with increasing mutations (due to higher genetic disorder). With every mutation, the value of α increases with an equidistant step: $\alpha_k = 0.3 + 2\cdot10^{-2}\cdot(k-1)$.

A similar relation was applied for the β-values: $\beta_k = 0.06 + 5\cdot10^{-3}\cdot(k-1)$. The values for k=1 represent the case of an adeno-carcinoma. From an immunological perspective, tumour sub-clones may develop in two different directions: Increasing mutations can lead to a better immunological elimination (due to the decreased expression of "don't eat me"-signals such as CD47 or inappropriate expression of other membrane-bound signalling molecules).

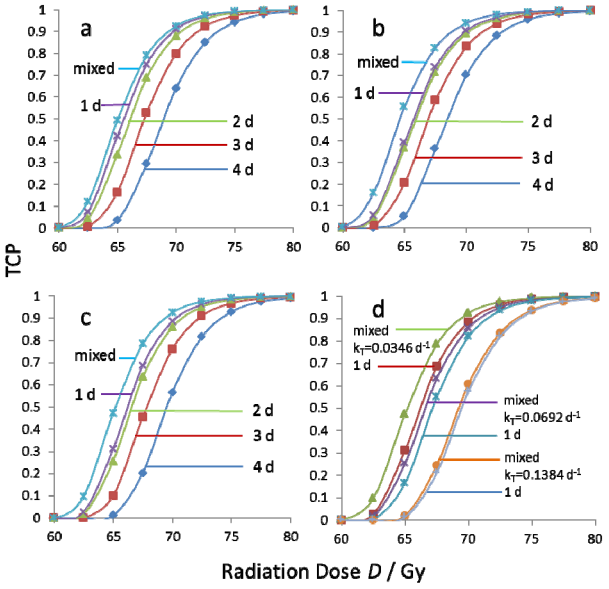

Figure 2: Tumour Control Probability TCP for a treatment of a tumour consisting on different sub-clones and different fractionation schemes (1 d = 1 day interval between fractions, 2 d = 2 days interval etc., mixed = 2 days interval between the initial 3 fractions, subsequent fractions in 1 day interval). (a) sub-clones with increasing weights w_k; (b) sub-clones with decreasing w_k; (c) single sub-clone scenario with average radio-sensitivity and (d) single sub-clone scenario with varying tumour doubling times.

The case with an enhanced immunological elimination for increasing k (with $k_{ime,k} = k\cdot k_{ime}$) is shown in Fig. 2a: Increased intervals between the fractions lead to a decreased tumour control (TCP-curves shifting to the right). The best tumour control can be achieved with the so called mixed protocol (first 3 fractions in an interval of 2 days, subsequent fractions daily). The explanation for this behaviour can be found by investigating the temporal development of the tumour cell population: After the first RT-fraction, a high amount of tumour cells are eliminated by radiation, leading to a high amount of apoptotic (or necrotic) cells. These cells are activating the immune response which in turn "co-eliminates" viable tumour cells. Depending on the selected invasion speed (governed by k_M), the elimination rate is low shortly after the end of irradiation, increases to a maximum after approxi-

mately 1 day and then decreases again. This effect can only be observed during the early (first to third) fractions. For the subsequent fractions, the immune system - mediated response becomes smaller due to the reduced amount of eliminated tumour cells and the radiation-induced elimination of immune cells during each irradiation. Therefore, repopulation (which is counteracting the immunological elimination) drives the outcome towards lower TCP-values, especially for larger intervals. This explains the lower tumour control for fractionation schemes having large intervals throughout the therapy course.

Decreasing immunological elimination (Fig. 2b) with incresing k ($k_{ime,k} = k^{-1} k_{ime}$) leads to similar results as in Fig. 2a. The effect of the mixed protocol is stronger compared to Fig. 2a and the difference between 1 day and 2 days interval is smaller, indicating the positive effect of immunological elimination during longer intervals at the beginning of the RT-course. It has to be pointed out here, that this result is influenced by the tumour evolution during the 300 days before therapy starts (initial conditions: $T_1(0) = 10^9$, $T_{k>1}(0) = 0$).

The comparison of the different cases (Fig. 2a & b) leads to the question how important the detailed modelling of different tumour sub-clones is. Fig. 2c shows a tumour where only one tumour population is taken into consideration. To achieve a comparable TCP, the radio-biological parameters are adapted to $\alpha_1 = 0.310\,\mathrm{Gy}^{-1}$ and $\beta_1 = 0.0625\,\mathrm{Gy}^{-2}$. The resulting TCP curve does not remarkably differ from the case exhibited in Fig. 2b, indicating a relatively small influence of the number of tumour cell populations considered in the model.

Since repopulation is counteracting the cell killing, simulations using different tumour doubling times (20 days, 10 days and 5 days) were carried out (Fig. 2d). The comparison of the mixed protocol with daily applied fractions reveals a disappearing therapeutic gain of the mixed protocol for fast repopulating tumours. This can be explained by the smaller decrease of the tumour cell population during the 2-day intervals compared to the case with slow repopulation. Especially during the second day of these intervals, faster repopulation compensates the immune-related elimination.

In Fig. 3, the response of one single tumour cell population onto the mixed protocol vs. daily fractions is shown for different conditions for repair and immunological elimination. The effect of incomplete repair leads to a strongly increased tumour control for both, mixed and daily fractionation. The difference between mixed and daily fractionation disappears at $\gamma = 2\ \mathrm{d}^{-1}$. The remaining dose equivalent Γ after one day interval is 0.4 Gy, representing moderate incomplete repair. With $\gamma = 1\ \mathrm{d}^{-1}$, the remaining dose equivalent Γ is 1.5 Gy. In this case, the mixed protocol exhibits a slightly lower TCP compared to the daily fractionation, indicating the strong influence of repair onto the outcome.

For an increased immunological elimination ($k_{ime} = 10^{-8}$) and incomplete repair (Fig. 3b), the mixed protocol reaches always higher TCP values, but the effect remains small. Fig. 3c shows the outcome for an increased immune cell density (governed by M_{max}). In this case, the effect of the mixed protocol becomes clearly larger for complete repair. For incomplete repair ($\gamma = 1\ \mathrm{d}^{-1}$), the difference between the two fractionation schemes remains small. Interestingly, this behaviour does not change when M_{max} is increased to 10^{13} and k_{ime} is set to 10^{-8} (Fig. 3d). The explanation for this small difference is the fact that after the first fraction of the treatment, the total number of tumour cells is reduced by over a factor 500 one day after irradiation. Therefore, subsequent fractions will not produce large amounts of apoptotic cells, resulting in a smaller activation of the immune system.

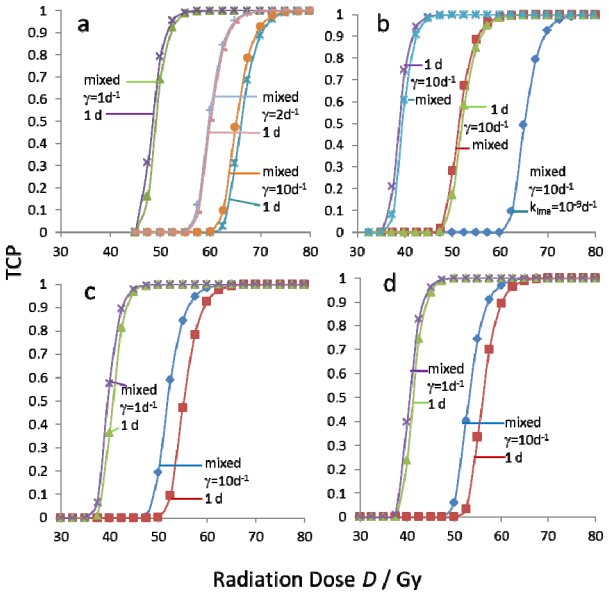

Figure 3: Tumour Control Probability TCP for a treatment of a tumour with varying repair speeds ($\gamma_k = \gamma = 1\ \mathrm{d}^{-1}$ = complete vs. ($\gamma = 2 \ldots 10\ \mathrm{d}^{-1}$ = incomplete repair) and varying immune-mediated elimination. Only mixed vs. daily fractionation is displayed. (a) $k_{ime} = 10^{-9}\ \mathrm{d}^{-1}$, $M_{max} = 10^9$; (b) $k_{ime} = 10^{-8}\ \mathrm{d}^{-1}$, $M_{max} = 10^9$; (c) $k_{ime} = 10^{-9}\ \mathrm{d}^{-1}$, $M_{max} = 10^{11}$; (d) $k_{ime} = 10^{-10}\ \mathrm{d}^{-1}$, $M_{max} = 10^{13}$.

Discussion and Conclusions

The presented model contains a simplistic approach to the tumour-immune system interaction. Therefore, the question is: What can we learn from such an artificial system *in silico*? Certainly, the presented model cannot be used as a predictive model, due to lack of any validation. Validation would require a comparison of model output to clinically observed TCP's and measuring immune cell densities during treatment.

The model includes an innate immune system type response and does not differentiate between the diverse populations of immune cells and their specific role in developing immune reaction. The interference with the adaptive immune response via antigen-presenting cells may strongly modify the tumour-specific response.

For assessing the kinetic constants, tumour-immune system interactions should be tracked during treatment to acquire time-resolved data. This is associated with big challenges even for a clinical trial and is not realistic in clinical routine. A

refinement of the immunological model would introduce a large number of additional parameters, many of them with large, patient-specific variations. To overcome these fundamental restrictions and difficulties, new approaches of modelling are needed. Looking to the immune system in its complexity, several network-structures involving signalling pathways and receptor signalling can be identified. Considering an adaptive immune system as a trainable network could lead to new insights to the dynamics of the tumour-immune-system interaction and – based on this - to new treatment concepts.

However, there are some concerns for modellers and clinicians as well. The process of modelling itself and simulations often helps to refine ideas and concepts about the investigated system. Regardless of the uncertainty concerning the parameter values, the range of parameter values was restricted to achieve more or less clinically realistic tumour control. In this range, the presented model depicts some aspects of the fundamental dynamics regarding innate immune system activation in combination with radiation-induced cell killing.

The model does not include competition between the tumour cell population and / or the host tissue, representing the situation of aggressive and fast growing tumours. In this regimen, considering different tumour sub-populations with varying radio-biological and immunological properties exhibits only a small influence on the tumour control, at least for the investigated parameter range. Detailed modelling of subclone – and host tissue interactions may become important when competition between the different populations reaches certain strength.

For description of the system, a compartmental model using ordinary differential equations is used. One may argue that some aspects of the ecosystem dynamics are related to the spatial distribution of cells / populations. Histological images from aggressive, highly malignant tumours often exhibit a more or less chaotic patchwork of host tissue, normoxic, hypoxic and necrotic areas, proliferating and apoptotic tumour cells etc.. Considering highly malignant tumours, the added value of spatio-temporal models is unclear. Therefore, the influence of spatial aspects in function of tumour malignancy on tumour evolution is an interesting and important research topic.

The general system behaviour exhibits the strong influence of repair on tumour control for the selected α – and β – values (representing a tumour with comparably high radio sensitivity). The reduced repair speed of tumour cells compared to the host tissue leads to a "therapeutic window" between TCP and Normal Tissue Complication Probability NTCP. No repair ($\gamma = 0\ d^{-1}$) will lead to survival which follows the linear-quadratic law, independent of fractionation. This results in a non-realistic TCP. Depending on the repair speed, immune system mediated response seems to be circumstantial compared to the cell-intrinsic radiation biology (incomplete repair). But for the most of the investigated cases (over a wide range of parameter values), the mixed protocol exhibits a slight and for stronger immune response a clear advantage compared to the daily applied fractions. In clinical practice, daily application of RT fraction is normally limited to Monday-Friday with an interruption every week end. This results in a "mixed" fractionation scheme, where the appearance of the larger intervals during treatment course is defined by the starting day of the treatment. It has to be pointed out that there are many other fractionation schemes such as hypo-fractionation (e.g. de Dios et al., 2017), brachytherapy or stereotactic radio-surgery, which may support the idea of a biological treatment planning using *in silico* - models.

There is some evidence for decreased tumour doubling time or increased rate of repopulation at the end of a treatment (Steel, 1977; Kim et al., 2005). This may be related to a smaller amount of tumour cells and related to this, less hypoxic cells or less competition. Another factor may be the selection of faster repopulating sub-clones during treatment course. The presented results are based on a constant tumour doubling. An accelerated growth at the end of RT treatment may be an additional argument for introducing longer intervals at the start of the treatment course.

For some indications, moderate hyperthermia is applied in combination with RT (HT-RT). In such therapy schemes, typically 3-6 RT-Fractions are combined with a hyperthermic treatment by heating the tumour tissue up to 42-43°C for 60-90 minutes. The effect of moderate hyperthermia in combination with Radiotherapy (HT-RT) was demonstrated in clinical trials (e.g. Wust et al. 2002) and experimentally in vitro and in vivo. Several mechanisms which potentially contribute to the treatment response have been discussed (Streffer, 1995). The impact of heat in combination with radiation on the level of the tumour ecosystem has not yet been investigated. Beside many other effects, hyperthermia leads to an increased tissue perfusion. This may result in an improved accessibility of immune cells (and to a changed tumour micro-environment). In combination with the heat-induced expression of heat-shock proteins (HSP), hyperthermia may enhance the intra-tumour immune cell activity leading to additional cell killing. An indication for the importance of this process is the fact that HT-RT seems to have improved clinical outcome with only a small number of combined HT-RT fractions compared to the total number of applied RT-fractions. Regarding the results presented above, it could be an interesting option to combine heating and irradiation with longer intervals at the beginning of the HT-RT course. For avoiding thermotolerance induction, HT-RT treatments are applied with a spacing of 3-7 days. This has to be taken into consideration for optimising treatment schemes. Population-based models for combined HT-RT such as the Multi-Hit Repair (MHR) model (Scheid-egger et al. 2013) can be integrated in the proposed frame-work to support therapy optimisation.

References

Abbott, R. G., Forrest, S., and Pienta, K. J. (2006). Simulating the Hallmarks of Cancer. *Artificial Life,* 12:617–634.

Baumann, M., Krause, M., Overgaard, J., Debus, J., Bentzen S.M., Daartz J. et al. (2016), Radiation oncology in the era of precision medicine. *Nat Rev Cancer,* 16(4):234-249.

Basanta, D., Anderson, A.R.A. (2015). Exploiting ecological principles to better understand cancer progression and treatment. *Interface Focus,* 3:20130020. http://dx.doi.org/10.1098/rsfs.2013.0020

Basanta, D., Gatenby, R.A., and Anderson, A.R. (2012). An exploiting evolution to treat drug resistance: combination therapy and the double bind. *Mol. Pharmaceut.,.* 9:914–921.

Bentley, K. (2013). Artificial life in the fight against cancer: Extended abstract of invited keynote lecture. In 2013 *IEEE Symposium on Artificial Life* (ALife), 145–147. doi:10.1109/ALIFE.2013.6602444

Chen, K.W., and Pienta, K.J. (2011). Modeling invasion of metastasizing cancer cells to bone marrow utilizing ecological principles. *Theoretical Biology and Medical Modelling,* 8:36.

Crespi, B., and Summers, K. (2005). Evolutionary biology of cancer. *Trends Ecol Evol,* 20:545–552. (doi:10.1016/j.tree.2005.07.007)

Daugaard, M., Rohde, and M., Jaattela, M. (2007). The heat shock protein 70 family: Highly homologous proteins with overlapping and distinct functions. *FEBS letters. 2007,* Jul 31;581(19):3702-10.

De Dios, N.R., Sanz, X., Foro, P., Membrive, I., Reig, A., Ortiz, A., Jiménez, R., and Algara, M. (2017). Accelerated hypofractionated radiation therapy (AHRT) for non-small-cell lung cancer: can we leave standard fractionation? *Clin Transl Oncol,* 19(4):440-447.

Fowler, J.F., and Ritter, M.A. (1995). A rationale for fractionation for slowly proliferating tumors such as prostatic adenocarcinoma. *Int J Radiation Oncology Biol. Phys.*, 32(2):521-529.

Gatenby, R.A., Gillies, R.J., and Brown, J.S. (2010). The evolutionary dynamics of cancer prevention. *Nat. Rev. Cancer,* 10:526–527. (doi:10.1038/nrc2892)

González-García, I., Solé, R. V., and Costa, J. (2002). Metapopulation dynamics and spatial heterogeneity in cancer. *Proc. Natl. Acad. Sci.,* U.S.A. 99:13085–13089.

Grimsley, C., and Ravichandran K.S. (2003). Cues for apoptotic cell engulfment: Eat-me, don't-eat-me, and come-get-me signals. *Trends in Cellular Biology*, 9:465.

Horsman, M.R., Mortensen, L.S., Petersen, J.B., Busk, M., and Overgaard J. (2012). Imaging hypoxia to improve radiotherapy outcome. *Nat. Rev. Clin. Oncol.,* 9(12):674-687.

Kim, J.J., and Tannock, I.F. (2005). Repopulation of cancer cells during therapy: an important cause of treatment failure. *Nature Reviews Cancer,* 5:517-525.

Maley, C. C. and Forrest, S. (2000). Exploring the Relationship between Neutral and Selective Mutations in Cancer. *Artificial Life,* 6:325–345.

Mehrara, E., Forssell-Aronsson, E., Ahlman, H., and Bernhardt, P. (2007). Specific growth rate versus doubling time for quantitative characterization of tumor growth rate. *Cancer Res.,* 67(8):3970-3975.

Merlo, L.M.F., Pepper, J.W., Reid, B.J., and Maley, C.C. (2006). Cancer as an evolutionary and ecological process. *Nat. Rev. Cancer,* 6:924–935. (doi:10.1038/nrc2013)

Nytko, K.J., Thumser-Henner, P., Weyland, M.S., Scheidegger, S., and Rohrer Bley, C. (in press). Sensitivity towards thermoradiotherapy treatment in canine and human cancer cell lines. *PLOS ONE*.

Ozik, J. et al. (2018). High-throughput cancer hypothesis testing with an integrated PhysiCell-EMEWS workflow. *BMC Bioinformatics,* 19:483.

Pienta, K.J., McGregor, N., Axelrod, R., and Axelrod, D.E. (2008). Ecological Therapy for Cancer: Defining Tumors Using an Ecosystem Paradigm Suggests New Opportunities for Novel Cancer Treatments. *Translational Oncology,* 1:158–164.

Scheidegger, S., Fuchs, H.U., Zaugg, K., Bodis, S., and Füchslin, R.M. (2013). Using State Variables to Model the Response of Tumour Cells to Radiation and Heat: A Novel Multi-Hit-Repair (MHR-) Approach. *Computational and Mathematical Methods in Medicine*, 2013, http://dx.doi.org/10.1155/2013/587543

Scheidegger, S, Lutters, G, and Bodis, S (2011a). A LQ-based kinetic model formulation for exploring dynamics of treatment response of tumours in patients. *Z. Med. Phys*., 21:164–173.

Scheidegger, S., and Füchslin, R.M. (2011b). Kinetic model for dose equivalent – an efficient way to predict systems response of irradiated cells. *Proc. of ASIM 2011,* (full papers, ISBN 978-3-905745-44-3).

Scheidegger, S., Lutters, G., and Bodis, S. (2010). Computer simulation of oxygenation and growth inhibition of tumours during fractionated radiotherapy: Exploration of the dynamic system behaviour. *Radiother. Oncol.,* 95, Suppl.1:512.

Scott, J.G., Fletcher, A.G., Anderson, A.R.A., and Maini P.K. (2016). Spatial metrics of tumour vascular organisation predict radiation efficacy in a computational model. *PLOS Comput Biol,* 12(1):e1004712. doi:10.1371/journal.pcbi.1004712

Steel, G. G. (1977). *The Growth Kinetics of Tumours*. Clarendon, Oxford.

Srivastava, S. (2002). Roles of heat-shock proteins in innate and adaptive immunity, *Nature Reviews Immunology,* 2:185-194.

Streffer, C (1995). Molecular and cellular mechanisms of hyperthermia. In: Seegenschmiedt, M.H., Fessenden, P., Vernon, C.C. (eds.), *Thermoradiotherapy and Thermochemotherapy*, pages 47-74, Springer Berlin, Heidelberg, New York.

Thorwarth, D. (2017). Biologically adapted radiation therapy. *Z Med Phys,* 28:177-183.

Van Leeuwen, C.M., Oei, A.L., Crezee, J., Bel, A., Franken, N.A.P, Stalpers, L.J.A., and Kok, H.P. (2018). The alpha and beta of tumours: a review of parameters of the linear-quadratic model derived from clinical radiotherapy studies. *Radiation Oncology,* 13:96, doi:10.1186/ s13014-018-1040-z

Vesely, M.D., Kershaw, M.H., Schreiber, R.D., and Smyth, M.J. (2011). Natural innate and adaptive immunity to cancer. *Annual Review of Immunology,* 29:235-271.

Wust, P, Hildebrandt, B, Sreenivasa, G, et al. (2002). Hyperthermia in combined treatment of cancer. *THE LANCET Oncology,* 3(8):487-497.

Zhang, L., Wang, Z., Sagotsky, J. A., and Deisboeck, T. S. (2009). Multiscale agent-based cancer modeling. *J. Math. Biol.,* 58:545–559.